The 8-Silyloxyquinoline Scaffold as a Versatile Platform for the Sensitive Detection of Aqueous Fluoride

ARTICLE *in* ANALYTICAL CHEMISTRY · APRIL 2015

Impact Factor: 5.64 · DOI: 10.1021/acs.analchem.5b00430 · Source: PubMed

4 AUTHORS, INCLUDING:

Xinqi Zhou
University of Nebraska at Lincoln
4 PUBLICATIONS **13** CITATIONS
SEE PROFILE

Rui Lai
University of Nebraska at Lincoln
2 PUBLICATIONS **9** CITATIONS
SEE PROFILE

analytical chemistry

Letter

pubs.acs.org/ac

The 8-Silyloxyquinoline Scaffold as a Versatile Platform for the Sensitive Detection of Aqueous Fluoride

Xinqi Zhou, Rui Lai, Hui Li, and Cliff I. Stains*

Department of Chemistry, University of Nebraska−Lincoln, Lincoln, Nebraska 68588, United States

Supporting Information

ABSTRACT: Utilizing a novel 8-silyloxyquinoline scaffold, we demonstrate the ability to synthesize fluorogenic probes for the sensitive and selective detection of inorganic fluoride (NaF) in aqueous samples. Our initial probe design (**2**) is capable of detecting inorganic fluoride at levels as low as 3.8 μM (72 ppb) in aqueous solutions, well below PHS recommended levels for drinking water (0.7−1.2 ppm), placing this probe among the most sensitive fluoride sensors reported to date. Furthermore, our results highlight the utility of the readily modifiable 8-silyloxyquinoline scaffold for the design of tailored fluoride sensing platforms. We demonstrate the ability to rationally tune the fluorescence and physical properties of the 8-silyloxyquinoline scaffold, producing a red-shifted fluoride probe (**4**) capable of detecting 50 μM (0.95 ppm) NaF in aqueous samples using a straightforward test-strip-based assay format. Taken together this work provides a template for the design of fluoride sensors capable of reporting on relevant concentrations of fluoride in the laboratory and in the field.

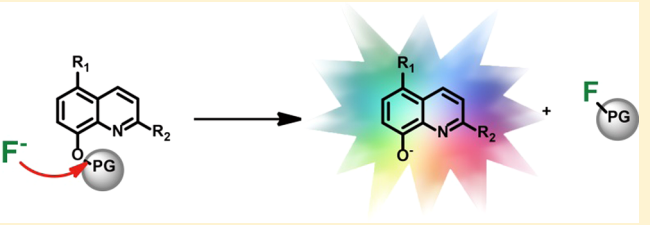

Numerous studies clearly document the beneficial role of fluoride in maintaining healthy teeth enamel, leading to the common practice of supplementing municipal water supplies and toothpaste with fluoride.[1,2] However, growing evidence also indicates that chronic overexposure to fluoride can lead to dental or skeletal fluorosis.[3,4] In particular, regions of endemic fluorosis are now well-described in underdeveloped countries.[5−8] Fluoride is also a product of the hydrolysis of sarin gas, further motivating the design of fluoride sensors. Current methodologies to quantify fluoride concentration in aqueous solutions, such as the Willard and Wilson method,[9] ion selective electrodes,[10] or ion chromatography[11] rely on time-consuming manipulations and high cost instrumentation. In contrast, recent advances in small molecule colorimetric-, fluorescent-, luminescent-, and electrochemical-based probes for fluoride could offer significant improvements in assay performance and cost.[12−25] However, the sensitive detection of fluoride in aqueous samples remains challenging due to the relatively high hydration enthalpy of fluoride in water (−121 kcal/mol).[26] As a consequence, although numerous fluoride sensing platforms have been described in the literature, these probes generally have detection limits in the mid micromolar range in aqueous samples (Supporting Information, Table S1). Given the current recommendations for fluoride levels in drinking water by the EPA (4 ppm or 211 μM) and PHS (0.7−1.2 ppm or 37−63 μM),[1] there is a pressing need for the development of chemosensors capable of quantifying fluoride at relevant concentrations in aqueous samples.

Small molecule fluoride sensors have commonly utilized the relatively strong hydrogen bonding potential of fluoride (38.6 kcal/mol) or the selective reaction of fluoride with Lewis acids in order to induce spectroscopic changes in small molecule probes.[19,20] Although powerful, hydrogen bond-based sensors often suffer from false positive signal generation in the presence of competing anions such as phosphate and acetate. On the other hand, the relatively strong interaction of fluoride with Lewis acids can be utilized to specifically detect fluoride when compared to potential competing anions. Utilizing this approach, Kim and Swager first described the use of silyl groups to selectively detect fluoride in organic solvents.[27] These probes rely on the dramatic difference in bond dissociation energies between Si−O and Si−F bonds, 103 versus 141 kcal/mol, respectively.[20] Indeed, numerous sensors have now been described based on the selective reaction of fluoride with silyl groups.[20] However, these silicon-based probes are generally limited in their application due to their analytical sensitivity in aqueous samples (Supporting Information, Table S1). Therefore, there is still a need for the fundamental investigation of probe structures employing the silicon-based Lewis acid approach to fluoride detection, with the long-term goal of enabling the sensitive quantification of fluoride in aqueous samples.

EXPERIMENTAL SECTION

General Reagents and Instrumentation. Unless otherwise noted, reactions were performed in oven-dried glassware under an inert atmosphere of N_2. All reagents and solvents were used as commercially supplied. Reaction progress was monitored by thin layer chromatography (TLC), and products

Received: February 1, 2015
Accepted: April 1, 2015

DOI: 10.1021/acs.analchem.5b00430
Anal. Chem. XXXX, XXX, XXX−XXX

were purified by flash chromatography using Merck silica gel 60 (230−400 mesh). ^{1}H NMR and ^{13}C NMR experiments were conducted in $CDCl_3$ under room temperature, and the spectra were recorded on Bruker-DRX-Avance 300 or 400 MHz instruments. Chemical shifts are reported relative to $CDCl_3$ (7.26 ppm for ^{1}H NMR and 77.0 ppm for ^{13}C NMR). Mass spectra were recorded using electrospray ionization mass spectrometry (ESI, Thermo Finnigan LCQ Advantage). Mass data are reported in units of m/z for $[M + H]^+$ or $[M + Na]^+$. Detailed synthetic procedures, characterization data, and computational results can be found in the Supporting Information. Fluorescence spectra were recorded on a FluoroMax-4 spectrofluorometer (Horiba Scientific) using 5 nm slit widths. UV−vis spectra were recorded using a BioMate 3S UV−visible spectrophotometer (Thermo Scientific). All absorbance assays were performed in 100 μL quartz cuvettes, and the fluorescence assays were performed in either 100 μL or 3.5 mL quartz cuvettes.

Determination of Molar Extinction Coefficients. TBAF (1 mM) was mixed with varying concentrations of the indicated sensor (0, 25, 50, 100, and 200 μM) in dioxane. Samples were allowed to react to completion with fluoride and the absorbance of each solution was measured. Molar extinction coefficients were determined from a linear fit of absorbance versus probe concentration.

Quantum Yield Measurements. The fluorescence quantum yields of **2** + F^- and **4** + F^- were determined using eq 1.

$$\Phi_x = (\Phi_{ST} \times A_{ST} \times F_X \times \eta_X^2)/(A_X \times F_{ST} \times \eta_{ST}^2) \quad (1)$$

where Φ is the quantum yield, A is the absorbance at the excitation wavelength (A was kept at ≤0.05 during fluorescence measurements in order to avoid self-quenching), F is the fluorescence intensity at the excitation wavelength, and η is the refractive index of the solvent. The subscripts ST and X refer to the standard and unknown, respectively. Quinine sulfate dihydrate (purchased from AnaSpec) in 0.5 M H_2SO_4 was used as the fluorescence reference standard, which has a quantum yield of 0.546 (ex. = 310 nm, em. = 455 nm). Quantum yields were measured in dioxane after reactions had progressed to completion in the presence of excess fluoride.

Absorbance and Fluorescence Assay Conditions. Sensors were mixed with the indicated concentrations of fluoride ion and were incubated at room temperature for 5 min in dioxane or 15 min in 50:50 (v/v) 10 mM HEPES (pH = 7.4):dioxane. Fluorescence was measured at the appropriate wavelengths for each probe (Table 1).

Selectivity of Probe 2. For the selectivity experiments shown in Figure 4, anions were prepared in 10 mM HEPES (pH = 7.4) at twice the final concentration in the assay. Sodium salts were used throughout, except for ClO_4^- where a TBA salt was used. Probe **2** was dissolved in dioxane at 40 μM. Anion solutions were mixed with dioxane in a 50:50 (v/v) ratio, and fluorescence was recorded after 15 min.

Table 1. Excitation and Emission Wavelengths for Fluoride Sensors in Nanometers

	2		4	
solvent	ex.	em.	ex.	em.
dioxane	345	536	346	553
50:50 (v/v) 10 mM HEPES (pH = 7.4):dioxane	393	542	N/A	N/A

A synthetic aquifer sample was prepared according to known concentrations of cations and anions found in the Minnelusa Aquifer located in South Dakota.[28,29] Final concentrations of species were 3.1 mM $CaSO_4$, 1.3 mM $MgSO_4$, 38 μM K_2SO_4, 4 mM $NaHCO_3$, 330 μM NaCl, 2.6 mM Na_2SO_4, and 3.75 μM NaBr. The fluoride concentration was adjusted to twice the indicated final concentration using NaF, and the resulting solution was mixed with an equal volume of 10 mM HEPES (pH = 7.4). Finally the buffered synthetic aquifer sample was mixed with dioxane (50:50, v/v) containg twice the final concentration of **2**. Fluorescence was recorded after 15 min.

Rate Constant Determination. Fluoride sensor **2** (20 μM) in a 50:50 (v/v) solution of HEPES buffer (10 mM, pH = 7.4):dioxane was spiked with 400, 800, 1200, 1600, or 2000 μM NaF. The reaction rate, k_{obs}, was obtained for each concentration of NaF by fitting the increase in fluorescence versus time using eq 2.

$$\text{fluorescence} = 1 - \exp(-k_{obs}t) \quad (2)$$

where t is time in minutes. The pseudo-first-order rate constant, k_{obs}, was then plotted against the concentration of NaF to yield the second-order rate constant using eq 3.

$$k_{obs} = k_2[\text{NaF}] \quad (3)$$

where k_2 is the second-order rate constant.

Test-Strip Assays. Filter paper (Whatman, 20 μm) was cut to 0.5 cm × 2 cm. Test strips were immersed into a dichloromethane (DCM) solution containing **4** (2 mM) and dried in air. To detect fluoride in water, the pretreated filter paper was immersed into an unbuffered DI water solution (containing 2 mM cetyltrimethylammonium bromide, CTAB) for 5 s and dried in air for 10 min. The fluorescence on the filter paper was observed and recorded under 365 nm using a hand-held UV lamp (UVGL-58 from UVP).

For selectivity assays with probe **4**, a synthetic aquifer sample was prepared with twice the final concentration of NaF desired in the assay. This sample was then mixed with 10 mM acetate (pH = 4.8) containing 2 mM CTAB at a 50:50 (v/v) ratio. The resulting solution was measured directly with test-strips of probe **4** as described in the preceding paragraph.

RESULTS AND DISCUSSION

Rational Design of an 8-Silyloxyquinoline-Based Fluoride Sensor. Given the ability of the 8-hydroxyquinoline scaffold to provide a sensitive fluorescent readout in aqueous samples,[30−33] we chose to investigate the ability of derivatives of this fluorophore to function as fluoride chemodosimeters. As an initial test of our approach, we envisioned the synthesis of a *tert*-butyldiphenylsilyl (TBDPS) protected 8-hydroxyquinoline (**2**) (Scheme 1). We hypothesized that cleavage of the TBDPS group in **2** by fluoride would result in the rapid formation of a fluorescent species. In addition, we reasoned that the carbonyl functionality present at position 2 of intermediate **1** would allow for facile modification in order to tune the spectral properties of our fluoride chemodosimeter platform. Lastly, we chose to include a sulfonamide at position 5 in sensor **2** as this functionality has been shown to dramatically increase the fluorescence of 8-hydroxyquinoline derivatives.[30]

We synthesized **2** according to Scheme 1 and investigated its response to fluoride by addition of 1 mM TBAF to a dioxane

DOI: 10.1021/acs.analchem.5b00430
Anal. Chem. XXXX, XXX, XXX−XXX

Scheme 1. Synthesis of 8-Silyloxyquinoline-Based Fluoride Sensor 2

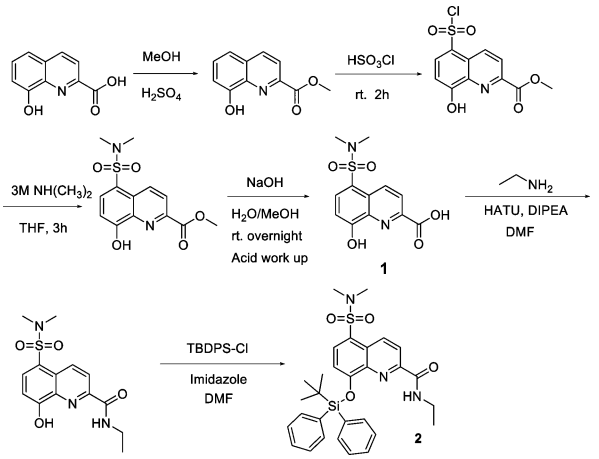

solution of **2**. Gratifyingly, we observed a marked change in both the absorbance and fluorescence emission spectra of the solutions upon addition of TBAF, producing a desilylated fluorescent product **3** (Supporting Information, Figure S1) with ε = 6600 M^{-1} cm^{-1} and Φ = 0.16 (Figure 1). Using a Job plot

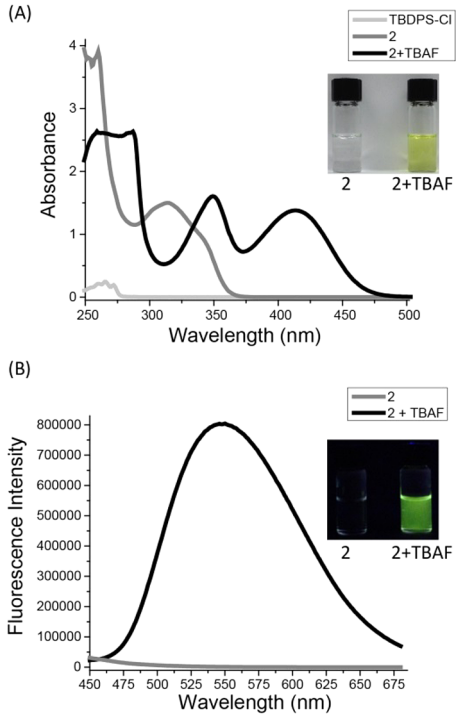

Figure 1. Absorbance (A) and fluorescence (B) of **2** (200 μM) in the absence or presence of 1 mM TBAF in dioxane; TBDPS-Cl is shown as a control. Fluorescence spectra were acquired by excitation at 345 nm.

we determined the stoichiometry of binding between **2** and fluoride to be 1:1 (Supporting Information, Figure S2), providing evidence for a detection mechanism in which one fluorine atom reacts with one molecule of **2** to produce TBDPS-F and a fluorescent species, **3**.

Computational Evaluation of Fluoride Detection by Probe 2. To better understand the molecular and electronic details of the detection mechanism, we performed density functional theory (DFT) and time-dependent DFT (TDDFT)[34,35] calculations for **2** and **3**. The 1,4-dioxane solvent was described by using the FixSol[36] solvation model (dielectric constant 2.25) implemented in the Quantum Chemistry Polarizable force field program (QuanPol)[37] integrated in the General Atomic and Molecular Electronic Structure System (GAMESS)[38,39] package. The B3LYP[40] functional and the 6-31++G(d,p)[41] basis set was used in both DFT and TDDFT calculations. The GAMESS TDDFT program implemented by Chiba et al.[42,43] was used together with the QuanPol FixSol model. We optimized the S_0 ground state geometries of **2** and **3** (Figure 2) using B3LYP and

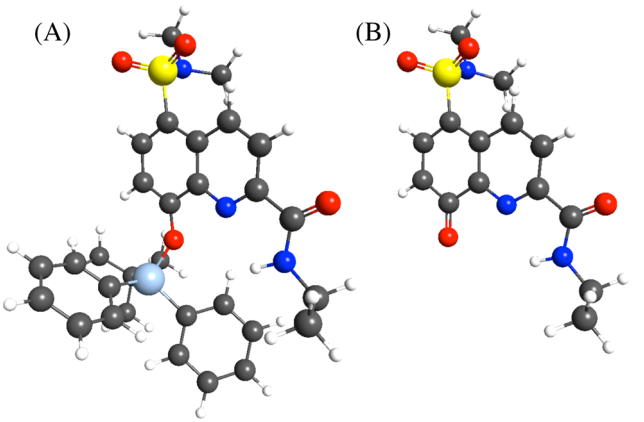

Figure 2. FixSol/B3LYP/6-31++G(d,p) optimized S_0 ground state geometries of **2** and **3** (A,B). FixSol/TD-B3LYP/6-31++G(d,p) optimized S_1 state geometries are similar, but some bond lengths are significantly different due to the electronic structure change.

performed single point energy calculations using TD-B3LYP to obtain the vertical excitation energies ($S_0 \rightarrow S_n$). Then we optimized the S_1 excited state geometries using TD-B3LYP and calculated the $S_1 \rightarrow S_0$ de-excitation energies (fluorescence). It was found that there are two significant absorptions at 340 and 258 nm (3.63 and 4.80 eV) and no significant fluorescence emission for **2**. There are six significant absorptions for **3**. The first one is at 425 nm (2.93 eV); the second one is at 350 nm (3.61 eV); the other four are at 264−273 nm (4.54, 4.56, 4.65, and 4.69 eV). The fluorescent emission of **3** is at 514 nm (2.41 eV). The full details of the computational results can be found in the Supporting Information. These calculated absorbance and emission spectra are in excellent agreement with experimental results (Figure 1), confirming the proposed mechanism of fluoride detection.

Limit of Detection and Selectivity of Fluoride Sensor 2. Confident in the mechanism of fluoride detection by **2**, we next investigated the limit of detection of **2** for TBAF in dioxane (Supporting Information, Figure S3). These data demonstrated the ability to resolve concentrations of TBAF as low as 0.56 μM (11 ppb). Building upon these promising results we next assessed the response of **2** to decreasing concentrations NaF in a 50:50 (v/v) solution of water:dioxane. These experiments revealed that **2** is capable of detecting as little as 3.8 μM or 72 ppb NaF in aqueous solutions, which is well below current guidelines for fluoride in drinking water (Figure 3).[1] Moreover, the limit of detection of **2** for inorganic fluoride in aqueous solutions is among the most sensitive of reported silyl-based fluoride sensors (Supporting Information, Table S1). We also interrogated the response of **2** to

DOI: 10.1021/acs.analchem.5b00430
Anal. Chem. XXXX, XXX, XXX−XXX

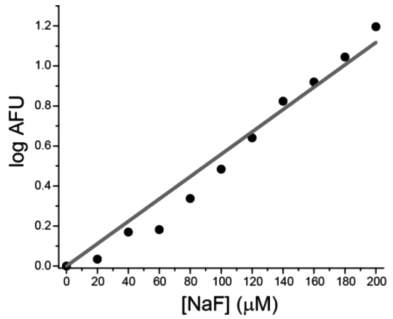

Figure 3. Emission of 20 μM **2** (at 542 nm) in a 50:50 (v/v) 10 mM HEPES (pH = 7.4):dioxane solution in the presence of the indicated concentration of NaF.

environmentally and biologically relevant anions. Impressively, we observed background levels of fluorescence for all anions in our panel except for fluoride. In addition, the response of **2** was not appreciably perturbed due to direct competition with any anion in our panel (Figure 4). We also interrogated the ability

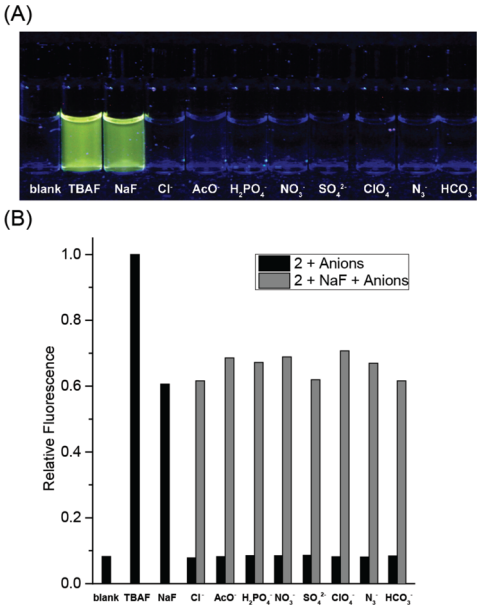

Figure 4. Selectivity of **2** (20 μM) for fluoride. (A) Images of **2**, under UV light, in the presence of the indicated anion (200 μM). (B) Black bars represent the fluorescence of **2** in the presence of the indicated anion (200 μM), while gray bars indicate the fluorescence of **2** in the presence of the indicated anion (200 μM) as well as NaF (200 μM). Assays were conducted in 50:50 (v/v) 10 mM HEPES (pH = 7.4):dioxane.

of **2** to report on the presence of NaF in a synthetic aquifer sample.[29] These experiments clearly demonstrate that environmentally relevant concentrations of cations and anions found in groundwater do not interfere with our assay (Supporting Information, Figure S4). Lastly, we assessed the rate of reaction of **2** with NaF, yielding a rate constant of 116 M^{-1} min^{-1} (Supporting Information, Figure S5). These data demonstrate the ability to rapidly detect fluoride in aqueous samples. Overall, the above experiments indicate the potential to utilize **2** for the sensitive laboratory detection of fluoride in water samples.

Test-Strip-Based Sensing of Fluoride in Aqueous Samples. Building upon these results, we envisioned a fluoride assay platform in which probe molecules would be adsorbed onto test-strips. We anticipated that these test-strips could then be utilized to measure fluoride concentrations in neat aqueous samples by monitoring the change in fluorescence of our probe. Such an assay format could allow for the point-of-use detection of fluoride. However, such an approach would require a fluoride chemosensor with low water solubility, ensuring that the probe would remain associated with the test-strip during subsequent analysis. We hypothesized that the ability to readily modify substituents on our fluoride sensing scaffold could yield a fluoride sensor with the desired physical properties. Accordingly, we appended an aniline substituent to **1** and protected this new fluoride sensor with TBDPS to afford fluoride sensor **4** (Scheme 2). As expected, addition of TBAF to a dioxane

Scheme 2. Synthesis of an Aniline Derivative of Fluoride Sensor 2

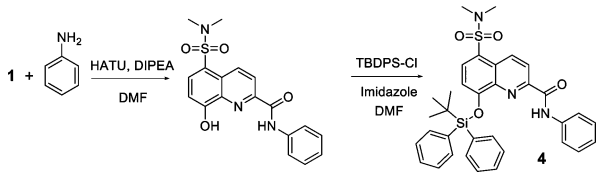

containing solution of **4** resulted in dramatic changes in the absorbance and emission spectra, producing a desilylated product with ε = 6330 M^{-1} cm^{-1} and Φ = 0.11 (Figure 5). Moreover, we observed a red-shift in the emission maxima of **4** compared to **2** in dioxane (553 versus 536 nm, respectively). In addition to these changes in the spectral properties of **4** compared to **2**, initial assays indicated that probe **4** was highly

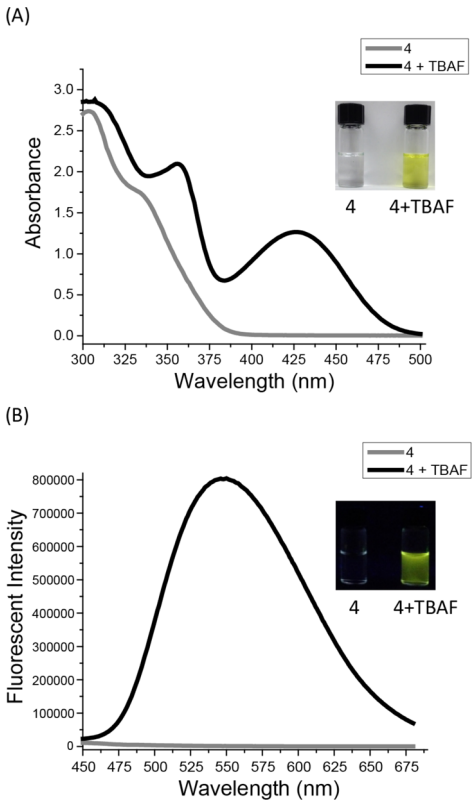

Figure 5. Absorbance (A) and emission spectra (B) of 200 μM **4** in the absence or presence of 1 mM TBAF in dioxane.

DOI: 10.1021/acs.analchem.5b00430
Anal. Chem. XXXX, XXX, XXX−XXX

insoluble in aqueous samples (data not shown). Taking advantage of the insolubility of **4** in aqueous solutions, we immersed filter paper strips in a DCM solution of **4**. These test-strips were dried and subsequently dipped into water samples containing increasing concentrations of NaF for 5 s. Test-strips were subsequently dried and imaged; clearly demonstrating the ability to detect fluoride at concentrations as low as 0.95 ppm (50 μM) using a straightforward assay format (Figure 6). This

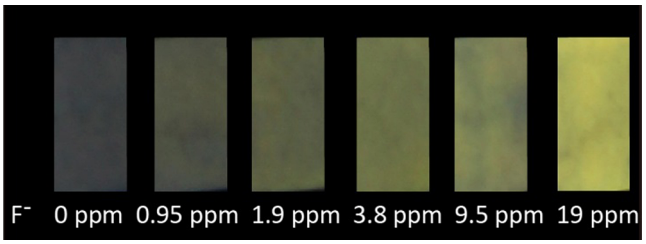

Figure 6. Fluorescence of test-trips containing **4** in the presence of the indicated concentration of NaF in water. Increasing fluorescence is observed with increasing NaF concentration.

test-strip-based assay was also capable of selectively detecting fluoride in a synthetic aquifer sample[29] (Supporting Information, Figure S6). These data indicate the potential of the 8-silyloxyquinoline scaffold as a versatile architecture for development of tailored fluoride sensing platforms. In the long term, the test-strip-based assay described above could be coupled with hand-held lateral fluorescence readers to enable the rapid detection of fluoride in the field.

CONCLUSIONS

In conclusion, we have demonstrated the versatility of the novel 8-silyloxyquinoline scaffold for the design of highly sensitive and selective platforms for the quantification of aqueous fluoride. Our initial fluoride sensor **2** can be utilized to detect fluoride in water samples, enabling the straightforward analysis of fluoride in the laboratory setting at concentrations well below the recommended levels in drinking water.[1] The poor water solubility of sensor **4** enabled the development of a test-strip-based assay for fluoride in aqueous samples that could potentially be utilized for the low-cost analysis of fluoride in the field. Taken together this work provides a readily modifiable, low-cost platform for the analysis of fluoride in water samples.

ASSOCIATED CONTENT

Supporting Information

Synthetic procedures, computational results, full characterization data for new compounds, and supporting data. This material is available free of charge via the Internet at http://pubs.acs.org.

AUTHOR INFORMATION

Corresponding Author

*E-mail: cstains2@unl.edu. Phone: 1-402-472-2617. Fax: 1-402-472-9402.

Notes

The authors declare no competing financial interest.

ACKNOWLEDGMENTS

We gratefully acknowledge the Department of Chemistry at the University of Nebraska−Lincoln for funding and the Research Instrumentation/NMR as well as Nebraska Center for Mass Spectrometry facilities for assistance in characterization of the new compounds. We also acknowledge helpful discussion with Prof. Rebecca Lai concerning synthetic aquifer samples.

REFERENCES

(1) Centers for Disease Control and Prevention. *Morbid. Mortal. Wkly. Rep.* **2001**, *50*, 1−42.
(2) Arnold, F. A., Jr.; Dean, H. T.; Jay, P.; Knutson, J. W. *Public Health Rep.* **1956**, *71*, 652−658.
(3) Krishnamachari, K. A. *Prog. Food Nutr. Sci.* **1986**, *10*, 279−314.
(4) Aoba, T.; Fejerskov, O. *Crit. Rev. Oral Biol. Med.* **2002**, *13*, 155−170.
(5) Irigoyen, M. E.; Molina, N.; Luengas, I. *Community Dent. Oral* **1995**, *23*, 243−245.
(6) Kloos, H.; Haimanot, R. T. *Trop. Med. Int. Health* **1999**, *4*, 355−364.
(7) Kodali, Y. R. R.; Krishnamachari, K. A. V. R.; Gowrinathsastry, J. *Trop. Doct.* **1994**, *24*, 136−137.
(8) Rawlani, S. *Indian J. Community Med.* **2010**, *35*, 298−301.
(9) Willard, H. H.; Winter, O. B. *Ind. Eng. Chem. Anal. Ed.* **1933**, *5*, 7−10.
(10) De Marco, R.; Clarke, G.; Pejcic, B. *Electroanalysis* **2007**, *19*, 1987−2001.
(11) van den Hoop, M. A. G. T.; Cleven, R. F. M. J.; van Staden, J. J.; Neele, J. *J. Chromatogr. A* **1996**, *739*, 241−248.
(12) Ashokkumar, P.; Weisshoff, H.; Kraus, W.; Rurack, K. *Angew. Chem., Int. Ed.* **2014**, *53*, 2225−2229.
(13) Cametti, M.; Rissanen, K. *Chem. Commun.* **2009**, 2809−2829.
(14) Guo, Z. Q.; Shin, I.; Yoon, J. *Chem. Commun.* **2012**, *48*, 5956−5967.
(15) Hirai, M.; Gabbai, F. P. *Angew. Chem., Int. Ed.* **2015**, *54*, 1205−1209.
(16) Hudnall, T. W.; Chiu, C. W.; Gabbai, F. P. *Acc. Chem. Res.* **2009**, *42*, 388−397.
(17) Ke, B.; Chen, W.; Ni, N.; Cheng, Y.; Dai, C.; Dinh, H.; Wang, B. *Chem. Commun.* **2013**, *49*, 2494−2496.
(18) Turan, I. S.; Akkaya, E. U. *Org. Lett.* **2014**, *16*, 1680−1683.
(19) Wade, C. R.; Broomsgrove, A. E.; Aldridge, S.; Gabbai, F. P. *Chem. Rev.* **2010**, *110*, 3958−3984.
(20) Zhou, Y.; Zhang, J. F.; Yoon, J. *Chem. Rev.* **2014**, *114*, 5511−5571.
(21) Li, L.; Ji, Y.; Tang, X. *Anal. Chem.* **2014**, *86*, 10006−10009.
(22) Swamy, P. C.; Mukherjee, S.; Thilagar, P. *Anal. Chem.* **2014**, *86*, 3616−3624.
(23) Aboubakr, H.; Brisset, H.; Siri, O.; Raimundo, J. M. *Anal. Chem.* **2013**, *85*, 9968−9974.
(24) Li, Y.; Duan, Y.; Zheng, J.; Li, J.; Zhao, W.; Yang, S.; Yang, R. *Anal. Chem.* **2013**, *85*, 11456−11463.
(25) Bozdemir, O. A.; Sozmen, F.; Buyukcakir, O.; Guliyev, R.; Cakmak, Y.; Akkaya, E. U. *Org. Lett.* **2010**, *12*, 1400−1403.
(26) Smith, D. W. *J. Chem. Educ.* **1977**, *54*, 540−542.
(27) Kim, T. H.; Swager, T. M. *Angew. Chem., Int. Ed.* **2003**, *42*, 4803−4806.
(28) Korshoj, L. E.; Zaitouna, A. J.; Lai, R. Y. *Anal. Chem.* **2015**, *87*, 2560−2564.
(29) Williamson, J. E.; Carter, J. M. *Water-Quality Characteristics in the Black Hills Area, South Dakota*, Water-Resources Investigations Report 01-4194; U.S. Geological Survey, Rapid City, SD, 2001.
(30) Pearce, D. A.; Jotterand, N.; Carrico, I. S.; Imperiali, B. *J. Am. Chem. Soc.* **2001**, *123*, 5160−5161.
(31) Shults, M. D.; Pearce, D. A.; Imperiali, B. *J. Am. Chem. Soc.* **2003**, *125*, 10591−10597.
(32) Beck, J. R.; Peterson, L. B.; Imperiali, B.; Stains, C. I. *Curr. Protoc. Chem. Biol.* **2014**, *6*, 135−156.
(33) Szalewski, D. A.; Beck, J. R.; Stains, C. I. *Bioorg. Med. Chem. Lett.* **2014**, *24*, 5648−5651.
(34) Casida, M. E. In *Recent Advances in Density Functional Methods*; Chong, D. P., Ed.; World Scientific: Singapore, 1995; p 155.

DOI: 10.1021/acs.analchem.5b00430
Anal. Chem. XXXX, XXX, XXX−XXX

(35) Casida, M. E.; Jamorski, C.; Casida, K. C.; Salahub, D. R. *J. Chem. Phys.* **1998**, *108*, 4439−4449.
(36) Thellamurege, N. M.; Li, H. *J. Chem. Phys.* **2012**, *137*, 246101.
(37) Thellamurege, N. M.; Si, D.; Cui, F.; Zhu, H.; Lai, R.; Li, H. *J. Comput. Chem.* **2013**, *34*, 2816−2833.
(38) Schmidt, M. W.; Baldridge, K. K.; Boatz, J. A.; Elbert, S. T.; Gordon, M. S.; Jensen, J. H.; Koseki, S.; Matsunaga, N.; Nguyen, K. A.; Su, S. *J. Comput. Chem.* **1993**, *14*, 1347−1363.
(39) Gordon, M. S.; Schmidt, M. W. In *Theory and Applications of Computational Chemistry: The First Forty Years*; Elsevier: Amsterdam, The Netherlands, 2005; pp 1167−1189.
(40) Becke, A. D. *J. Chem. Phys.* **1993**, *98*, 5648−5652.
(41) Francl, M. M.; Pietro, W. J.; Hehre, W. J.; Binkley, J. S.; Gordon, M. S.; DeFrees, D. J.; Pople, J. A. *J. Chem. Phys.* **1982**, *77*, 3654−3665.
(42) Chiba, M.; Tsuneda, T.; Hirao, K. *J. Chem. Phys.* **2006**, *124*, 144106−144111.
(43) Chiba, M.; Tsuneda, T.; Hirao, K. *Chem. Phys. Lett.* **2006**, *420*, 391−396.

DOI: 10.1021/acs.analchem.5b00430
Anal. Chem. XXXX, XXX, XXX−XXX